



## **Experimental, density functional computations of the vibrational Spectra, NBO analysis and HOMO–LUMO of trioxsalen**

**N.Swarnalatha<sup>\*1</sup>, S. Gunasekaran<sup>2</sup>, S. Muthu<sup>3</sup>**

<sup>1</sup>Department of Physics, SCSVMV University, Enathur, Kanchipuram 631561, Tamil Nadu, India.

<sup>2</sup>Research and Development, St. Peter's Institute of Higher Education and Research, St. Peter's University, Avadi, Chennai 600054, Tamil Nadu, India

<sup>3</sup>Department of Physics, Sri Venkateswara College of Engineering, Sriperumbudur 602117, Tamil Nadu, India.

**Abstract:** In this work, the vibrational spectra of trioxsalen by experimental and quantum chemical calculations of trioxsalen was reported. The solid phase FT-Raman and FT-IR spectra of the title compound were recorded in the region 4000 cm<sup>-1</sup> to 100 cm<sup>-1</sup> and 4000 cm<sup>-1</sup> to 400 cm<sup>-1</sup> respectively. The harmonic vibrational frequencies have been calculated by using density functional theory (DFT) B3LYP method with standard 6-311++ G(d,p) basis set. The vibrational assignments were performed on the basis of potential energy distribution (PED) of the vibrational modes. The stability of the molecule, arising from hyper conjugative interactions and charge delocalization have been analysed using natural bond orbital (NBO). The calculated HOMO and LUMO energies show that charge transfer occurs within the molecule.

**Key words:** DFT, FT-IR, FT-Raman, NBO, HOMO-LUMO.

### **Introduction**

Trioxsalen is one of the photosensitizing furanocoumarin and a psoralen derivative, which on photoactivation stimulate melanocytes and induce their proliferation. It is used in the treatment of psoriasis. The compatibility of trioxsalen was evaluated with pharmaceutical excipients used in the solid forms based on the DTA (Differential Thermal Analysis) and DSC (Differential Scanning Calorimetry) results<sup>1</sup>. The study of PUVA therapy combines UV-A light with trioxsalen carried out by Maïamet al<sup>2</sup>. A method using high performance liquid chromatography (HPLC) and liquid chromatography tandem mass spectrometry (LC-MS/MS) was developed with trioxsalen in cosmetics<sup>3</sup>. Patients with psoriasis were treated using trioxsalen bath and long wave ultraviolet (UVA) and obtained good results<sup>4</sup>. Penetration of trioxsalen into the skin was studied by Niilovaatainen et al.<sup>5</sup>. The quantitative determination of trioxsalen in human plasma by glass Capillary Gas Chromatography Mass spectrometry was investigated in the pictogram range by Taskinen et al<sup>6</sup>.

### **Experimental details**

The compound under investigation, namely trioxsalen was purchased from Sigma Aldrich chemical company with a stated purity of 99% and it was used as such without further purification. The FT-IR spectrum of the molecule was recorded in the region 4000-400 cm<sup>-1</sup> on IFS 66V spectrophotometer using the KBr pellet technique. The FT-Raman spectrum of the molecule was recorded in the region 4000-100 cm<sup>-1</sup> in the pure mode using Nd:YAG Laser of 100 mW on a BRUCKER RFS 27 at SAIF, IIT, Chennai, India.

## Computational details

Quantum chemical calculations of the title compound are carried out with Gaussian03 program<sup>7</sup>Becke's three parameter exchange functional (B3)<sup>8,9</sup> and combined with the correlation functions of Lee, Yang and Parr (LYP), with standard 6-311++G(d,p) basis set. The spectra were analyzed in terms of the PED contributions by using the VEDA program<sup>10</sup>.HOMO and LUMO energies and natural bonding orbital (NBO) calculations are performed using Gaussian 03 program at the DFT level using 6-311++G(d,p) basis set in order to understand various second order interactions between the filled orbital of the intermolecular delocalization or hyper conjugation.

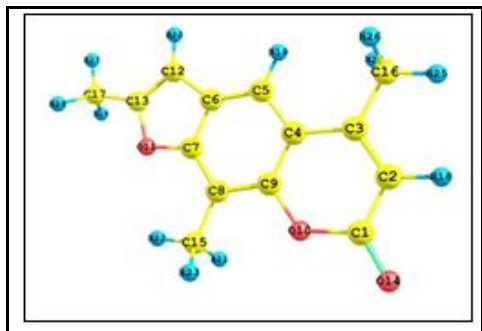


Figure 1. Atom numbering system adopted in this study for trioxsalen.

## Results and Discussions

### Vibrational analysis

In our present study, we have performed a frequency calculation analysis to obtain the spectroscopic signature of trioxsalen. The trioxsalen molecule consists of 29 atoms and they have 81 vibrational normal modes. All the frequencies are assigned in terms of fundamental, overtone and combination bands. The optimized structure of the title molecule in accordance with the atom numbering scheme is shown in Figure.1. Assignments have been made on the basis of potential energy distribution (PED). The measured (FT-IR and FT-Raman) wave numbers and assigned wave numbers of the some selected intense vibrational modes calculated at B3LYP level with 6-311++G(d,p) basis set along with their PED are given in Table 1. This reveals good correspondence between theory and experiment in main spectral features.

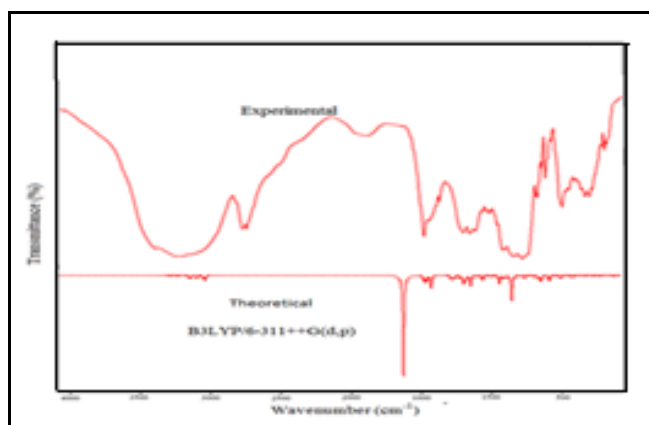


Figure 2. Experimental and calculated FT-IR spectrum of trioxsalen.

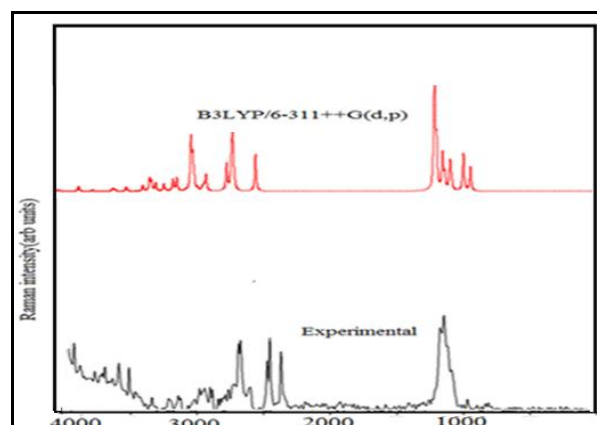


Figure 3. Experimental and calculated FT-Raman spectrum of trioxsalen.

Table 1. Calculated scaled IR wavenumbers, relative intensities for trioxsalen using B3LYP/6-311++G(d,p) basis set.

Mode No	Experimental (cm <sup>-1</sup> )		Calculated Frequencies <sup>a</sup> (cm <sup>-1</sup> )			Vibrational assignments PED (%)
	FT-IR	FT - Raman	Scaled	IR <sub>int</sub> <sup>b</sup>	Raman <sub>int</sub> <sup>c</sup>	
1		3133	3136.65	0.57	24.07	γCH(99)
2	3100	3099	3097.33	0.21	28.67	γCH(99)
3	3095	3096	3093.92	0.39	11.95	γCH(99)
4	-	3041	3028.00	0.86	8.44	γCH(100)
5	-	-	3020.25	1.08	16.79	γCH(99)
6	-	3018	3016.76	2.14	15.54	γCH(99)
7	-	-	2987.95	1.04	14.03	γCH(100)
8	2976	-	2977.17	1.09	11.72	γCH(100)
9	2957	2975	2975.00	1.13	25.89	γCH(100)
10	2935	2960	2940.49	1.80	40.61	γCH(100)
11	2929	2917	2929.09	1.35	37.76	γCH(100)
12	2917	2919	2928.18	3.50	100.00	γCH(99)
13	1776	-	1732.87	100.00	36.90	γOC(85)
14	1612	1612	1609.62	5.74	8.52	γCC(80)
15	1603	1600	1600.77	0.04	47.39	γCC(71)
16	1593	1592	1593.89	5.94	30.18	γCC(75)
17	1574	1536	1565.88	12.43	26.94	γCC(70)
18	-	1465	1449.20	0.35	2.24	γCC(75)
19	1451	1463	1446.39	2.44	13.42	βHCH(65)
20	-	1424	1441.93	0.99	1.17	βHCH(75)
21	1436	1403	1436.33	0.91	1.31	βHCH(81)+τHCCC(11)
22	-	-	1434.93	1.20	1.63	βHCH(85)
23	1432	1430	1430.65	1.31	2.77	βHCH(32)
24	1420	1421	1423.25	1.07	2.35	βHCH(80)
25	1393	1392	1397.43	2.07	2.54	γCC(11)+βHCC(65)
26	1370	1377	1377.10	2.21	10.45	βHCH(45)
27	-	-	1370.36	0.51	5.36	βHCH(90)
28	1369	1369	1369.20	6.67	23.34	βHCH(35)
29	1350	1343	1359.35	3.67	50.28	βHCH(21)+βCCC(45)

30	1325	1301	1328.93	10.53	1.03	$\gamma_{CC}(75)+\beta_{HCC}(25)$
31	1295	1284	1277.56	1.23	12.98	$\beta_{CCO}(25)+\beta_{HCC}(65)$
32	1258	1278	1254.88	4.57	11.61	$\gamma_{CC}(15)+\gamma_{OC}(30)+\beta_{HCC}(30)$
33	1211	1224	1214.94	0.32	0.72	$\gamma_{CC}(25)+\gamma_{OC}(35)$
34	1200	1225	1202.28	0.83	7.04	$\beta_{HCC}(60)$
35	1165	1181	1155.24	8.10	8.15	$\gamma_{CC}(75)$
36	1145	1164	1130.51	2.33	9.43	$\gamma_{CC}(50)+\beta_{HCC}(35)$
37	1130	1122	1119.51	1.60	12.04	$\gamma_{CC}(35)+\beta_{HCC}(35)$
38	-	1085	1080.77	24.82	5.69	$\gamma_{OC}(35)+\tau_{HCCC}(35)$
39	1041	1049	1041.97	0.07	0.27	$\gamma_{CC}(50)+\beta_{COC}(35)$
40	1032	-	1027.55	0.17	0.11	$\beta_{HCH}(80)+\tau_{HCCC}(15)$
41	1030	1025	1024.75	0.25	0.10	$\beta_{HCH}(25)+\tau_{HCCC}(65)$
42	1015	1020	1020.88	0.00	0.00	$\beta_{HCH}(40)+\tau_{HCCC}(53)$
43	1003	1008	1003.89	2.21	0.14	$\beta_{HCH}(20)+\tau_{HCCC}(50)$
44	985	994	984.22	0.26	4.07	$\gamma_{CC}(15)+\beta_{HCH}(15)+\tau_{HCCC}(50)$
45	940	943	946.25	1.31	0.15	$\gamma_{CC}(30)+\beta_{CCC}(40)$
46	925	925	917.92	3.04	2.21	$\gamma_{OC}(45)$
47	906	904	905.36	5.77	2.55	$\gamma_{OC}(25)$
48	854	852	854.50	5.49	0.14	$\tau_{HCCC}(85)$
49	842	840	839.67	0.01	0.18	$\tau_{HCCC}(70)$
50	802	807	808.04	0.29	0.16	$\gamma_{OC}(45)$
51	778	780	789.33	1.35	1.50	$\gamma_{CC}(25)+\beta_{OCO}(20)+\beta_{CCC}(20)$
52	780	782	782.59	1.76	0.11	$\tau_{HCCC}(80)$
53	734	727	727.48	1.28	0.08	$\tau_{HCCC}((45)+\tau_{COCC}(15)$
54	704	720	706.00	1.08	4.92	$\beta_{CCO}(15)+\tau_{COCC}(15)+\gamma_{OCOC}(35)$
55	708	705	708.06	0.05	0.08	$\beta_{CCC}(25)$
56	665	665	668.91	0.14	0.05	$\tau_{CCCC}(20)+\gamma_{COCC}(25)+\gamma_{OCOC}(28)+\gamma_{OCCC}(15)$
57	628	-	635.45	0.52	0.34	$\gamma_{OC}(15)+\gamma_{CC}(25)+\beta_{CCO}(20)$
58	607	600	604.24	0.13	0.62	$\tau_{CCOC}(48)+\tau_{COCC}(20)+\gamma_{CCOC}(20)$
59	589	579	586.87	0.68	1.51	$\beta_{OCO}(26)+\beta_{CCC}(30)$
60	552	554	553.38	0.15	0.23	$\tau_{HCCC}(10)+\gamma_{CCCC}(20)+\tau_{OCCC}(22)$
61	562	550	550.99	0.78	0.21	$\beta_{CCC}(11)+\beta_{CCO}(15)+\beta_{OCC}(20)$
62	534	-	535.72	0.24	4.89	$\gamma_{CC}(55)+\beta_{CCC}(25)$

63	490	478	474.26	0.16	0.10	$\tau\text{CCCC}(26)+\gamma\text{CCCC}(30)+\gamma\text{OCCC}(25)$
64	465	-	465.65	0.73	0.48	$\gamma\text{CC}(25)+\beta\text{CCC}(25)+\beta\text{CCO}(20)$
65	420	430	414.38	0.97	1.67	$\gamma\text{CC}(25)+\beta\text{OCO}(20)+\beta\text{COC}(20)+\beta\text{CCO}(15)$
66	-	373	371.48	0.04	0.04	$\tau\text{CCCC}(11)+\tau\text{COCC}(17)+\beta\text{OCCC}(21)+\beta\text{OCCC}(10)$
67	-	353	358.62	0.18	2.12	$\beta\text{CCC}(22)+\beta\text{CCO}(20)+\beta\text{CCC}(30)$
68	-	330	330.12	0.15	0.62	$\gamma\text{CC}(25)+\beta\text{OCO}(11)+\beta\text{CCO}(15)+\beta\text{CCC}(22)$
69	-	320	320.95	0.15	0.09	$\tau\text{CCCC}(20)+\text{COCC}(10)+\gamma\text{CCOC}(16)+\gamma\text{CCCC}(25)$
70	-	297	276.79	0.00	0.58	$\beta\text{CCC}(45)$
71	-	225	224.20	0.00	0.11	$\tau\text{CCCC}(17)+\tau\text{CCOC}(13)+\tau\text{COCC}(10)+\beta\text{CCOC}(15)$
72	-	210	215.77	0.31	0.06	$\beta\text{OCC}(16)+\beta\text{CCC}(50)$
73	-	-	201.79	0.15	0.16	$\tau\text{HCCC}(65)+\tau\text{CCOC}(30)$
74	-	187	169.52	0.43	0.04	$\tau\text{CCCC}(27)+\beta\text{CCCC}(30)$
75	-	-	168.17	0.02	0.15	$\beta\text{OCC}(65)+\beta\text{CCO}(25)$
76	-	160	158.24	0.03	0.15	$\beta\text{OCC}(25)+\beta\text{CCC}(50)$
77	-	141	139.70	0.08	0.02	$\beta\text{CCC}(50)+\tau\text{HCCC}(65)$
78	-	112	132.61	0.01	0.12	$\beta\text{CCOC}(30)+\tau\text{HCCC}(45)$
79	-	77	79.47	0.34	0.07	$\gamma\text{CC}(25)+\beta\text{CCC}(20)+\tau\text{HCCC}(45)$
80	-	67	66.14	0.00	0.09	$\tau\text{HCCC}(45)+\tau\text{CCOC}(20)+\tau\text{HCCC}(11)+\tau\text{CCCO}(15)$
81	-	54	55.78	0.09	0.03	$\tau\text{HCCC}(65)+\tau\text{CCOC}(20+)+\beta\text{OCCC}$

IR int b IR intensity (Kmmol<sup>-1</sup>)

Raman intensity (arb.units)

 $\gamma$  - stretching,  $\beta$  - in plane bending,  $\gamma$  - out of plane bending,  $\tau$  - torsion a Scaling factor: 0.967 for DFT (B3LYP)/6-311++G (d,p) basis set

b Relative absorption intensified and normalised with highest peak absorption = 100.

### C-H vibrations

The hetero aromatic structure shows the presence of C-H stretching vibrations in the region 3100–3000  $\text{cm}^{-1}$ , which is the characteristic region for the ready identification of trioxsalen vibrations<sup>11</sup>. In this region, the bands are not affected, appreciably by the Nature of the substituents. In the FT-Raman spectrum of trioxsalen is observed at 3100, 3095, 2976, 2957, 2935, 2929, 2917  $\text{cm}^{-1}$  are assigned to C-H stretching vibrations. This mode is calculated in the range 3136-2928  $\text{cm}^{-1}$  with B3LYP / 6-311++G(d,p) method. As expected these modes are pure stretching modes as it evident from a PED column in Table 1. The C-H in-plane bending frequencies appear in the range 1300–1000  $\text{cm}^{-1}$  and are very useful for characterization purpose. In this work, the in-plane bending vibrations were observed at 1393, 1370, 1200, 1130  $\text{cm}^{-1}$  in FT-IR spectrum and at 1392, 1377, 1225, and 1122  $\text{cm}^{-1}$  in FT-Raman spectrum. The PED of vibrations shows that they are not in pure modes. The theoretically scaled vibrations with B3LYP/6-311++G (d,p) method, also shows good agreement with experimentally recorded data. The C-H out-of-plane bending vibrations are strongly coupled vibrations and occur in the region 1000–750  $\text{cm}^{-1}$ . In this work, the out-of-plane bending vibrations were recorded at 854 and 842  $\text{cm}^{-1}$  in FT-IR spectrum and at 852 and 840  $\text{cm}^{-1}$  in FT-Raman spectrum.

### C=O vibrations and C-O vibrations

The C=O stretch of carboxylic acids is identical to the C=O stretch in ketones, which is expected in the region 1740–1660  $\text{cm}^{-1}$ <sup>12</sup>. The band is reasonably easy to be recognized due to its high intensity. In the present study the band observed at 1776  $\text{cm}^{-1}$  in FT-IR and 1760  $\text{cm}^{-1}$  in FT-Raman is assigned for C=O vibration and it coincides with calculated value as 1734  $\text{cm}^{-1}$  with PED contribution of 85%. This multiple bonded group is highly polar and therefore gives rise to an intense infrared absorption band. In the C-O bond, the absorption is sensitive for both the carbon and oxygen atoms of the carbonyl group. We can find that the C-O vibration has been affected by the neighboring molecular interactions. Normally it occurs in the region 1260–1000  $\text{cm}^{-1}$ <sup>13,14</sup>. However, these bands overlap with other bands that are due to aromatic vibrations causing that their undisputed assignment is often difficult. In the present case, the bands at 925, 906  $\text{cm}^{-1}$  in FT-IR spectrum and 925, 904  $\text{cm}^{-1}$  in FT-Raman spectrum are assigned to C-O vibrations which agrees with calculated values at 917 and 905  $\text{cm}^{-1}$  with a PED contribution of 70%, 85% respectively. These assignments are in good agreement with the literature value.

### C-C vibrations

The carbon–carbon stretching modes of the phenyl group are expected in the range from 1650 to 1200  $\text{cm}^{-1}$ . The actual position of these modes is determined not so much by the nature of the substituent but by the form of substitution around the ring<sup>15</sup>. In general, the bands are of variable intensity and are observed at 1258, 1211, 1200, 1165, 1145, 1130  $\text{cm}^{-1}$  in FT-IR spectrum and 1278, 1224, 1225, 1181, 1164, 1122, 1085, 1049  $\text{cm}^{-1}$  in FT-Raman spectrum respectively. The theoretically computed values of C-C vibrations are 1255, 1245, 1202, 1155, 1131, 1120, 1081, 1402  $\text{cm}^{-1}$  with almost 80% of PED contribution.

### NBO analysis

A useful aspect of the NBO method is that it gives information about interactions in both filled and virtual orbital spaces that could enhance the analysis of intra- and intermolecular interactions. The second-order Fock matrix was calculated to evaluate the donor–acceptor interactions in NBO analysis<sup>16</sup>. The interactions result in a loss of occupancy from the localized NBO of the idealized Lewis structure in an empty non-Lewis orbital. For each donor (i) and acceptor (j), the stabilization energy  $E_2$  associated with the delocalization  $i \rightarrow j$  is estimated as

$$E_2 = \Delta E_{ij} = \frac{q_i (F_{ij})^2}{\epsilon_j - \epsilon_i}$$

Where  $q_i$  is the donor orbital occupancy,  $\epsilon_j$  and  $\epsilon_i$  are diagonal elements and  $F_{ij}$  is the off diagonal NBO Fock matrix element.

The NBO analysis gives a convenient basis for investigating charge transfer or conjugative interaction in molecular systems. Some electron donor orbital, acceptor orbital and the interacting stabilization energies resulting from the second-order micro-disturbance theory are reported<sup>17</sup>. The larger the  $E(2)$  value, the more intensive is the interaction between electron donors and electron acceptors, i.e., the more donating tendency from electron donors to electron acceptors and the greater the extent of conjugation of the whole system. Delocalization of electron density between occupied Lewis-type (bond or lone pair) NBO orbital and formally unoccupied (antibond or Rydberg) non-Lewis NBO orbital corresponds to a stabilizing donor–acceptor interaction. NBO analysis was performed on the title molecule at B3LYP/6-311++G (d,p) level in order to elucidate the intramolecular, hybridization and delocalization of electron density in the title molecule and were

presented in Table 2. The atoms of  $\pi$ (C1-O14) to  $\pi^*$ (C2-C3) with stabilization energy of 3.13 kJ/mol and from  $\pi$ (C5-C6) to  $\pi^*$ (C4-C9) antibonding orbitals with stabilization energy of 17.99 kJ/mol. From  $\sigma$ (C17-H28) to  $\sigma^*$ (C17-H28) with stabilization energy of 0.67 kJ/mol. The magnitude of energy transferred from LP (2) of O10  $\rightarrow \sigma^*$ (C1-C2) had the stabilization energies 1.07 kJ/mol. Similarly the electron donated from LP (2) O15  $\rightarrow \sigma^*$ (C17-H29) leads to the stabilization energy of 2.73 KJ/mol.

**Table 2. Second order perturbation theory analysis for trioxsalen using B3LYP/6-311++G(d,p) basis set.**

Donor (i)	Type	ED (i)(e)	Acceptor (j)	Type	ED (j)(e)	E(2) <sup>a</sup> (kJ/mol)	E(j) - E(i) <sup>b</sup> (a.u)	F (i,j) <sup>c</sup> (a.u)
C 1 - O 14	$\Pi$	1.98466	C 2 - C 3	$\pi^*$	0.1361	3.13	0.45	0.035
C 5 - C 6	$\Pi$	1.97422	C 4 - C 9	$\pi^*$	0.46158	17.99	0.27	0.064
C 13 - C 17	$\Sigma$	1.98834	C 15 - H 23	$\sigma^*$	0.00919	23.78	0.98	0.136
C 17 - H 28	$\Sigma$	0.01201	C 17 - H 28	$\sigma^*$	0.01197	0.67	3.02	0.04
O 10	LP ( 2)	1.77173	C 1 - C 2	$\sigma^*$	0.0626	1.07	0.71	0.026
O 14	LP ( 2)	1.85831	C 17 - H 29	$\sigma^*$	0.01197	2.73	3.82	0.094

### Homo – Lumo energy gap

The concepts of aromaticity, HOMO and LUMO are of fundamental importance in understanding the chemical stability and reactivity of many organic molecules. Molecular orbital and their properties like energy is very useful to the physicists and chemists and their frontier electron density is used for predicting the most reactive position in p electron system and also explains several types of reaction in conjugated systems<sup>18</sup>. Both the HOMO and LUMO are the main orbitals which take part in chemical stability. HOMO represents the ability to donate an electron, LUMO as an electron acceptor, represents the ability to obtain an electron. Moreover, the Eigenvalues of the HOMOs (p donor) and the LUMOs (p acceptor) and their energy gap reflects the chemical activity. Recently, the energy gap between HOMO and LUMO has been used to prove the bioactivity from intra-molecular charge transfer (ICT)<sup>19,20</sup>. The calculated energy values for HOMO and LUMO energies are -0.212 a.u and -0.056 a.u respectively. The difference in energies of HOMO and LUMO is 0.155 a.u respectively. The 3D plots of HOMO and LUMO of trioxsalen are shown in Figure 4.

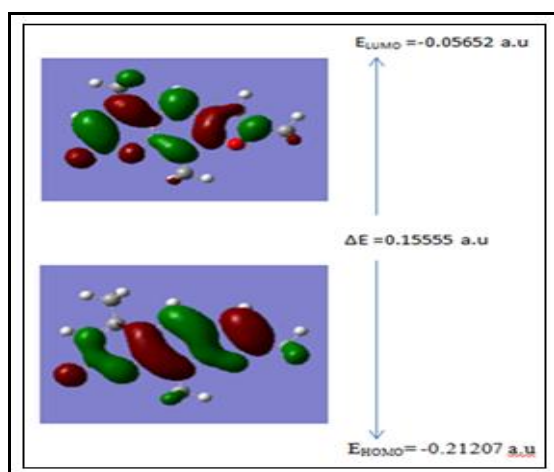


**Figure 4. The HOMO, LUMO orbitals of trioxsalen at B3LYP/6-311++ density functional calculations**

### Conclusion

The spectral studies such as FT-IR, FT-Raman for trioxsalen was carried out with quantum chemical computations. A complete vibrational and molecular structure analysis has been performed based on the quantum mechanical approach by B3LYP calculations in 6-311++G(d,p) basis set. The difference between the observed and scaled wave number values of the most of the fundamental is very small. The complete vibrational assignment with PED was calculated. The theoretically constructed FT-IR and FT-Raman spectra had good correlation with experimentally observed FT-IR and FT-Raman spectra. NBO analysis was made and

it indicated the intra molecular charge transfer between the bonding and antibonding orbitals. The calculated HOMO and LUMO energies were used to analyze the charge transfer within the molecule.

## References

1. NGPB, LimaIPB, Barros DMC,OliveiraTS, Raffin FN, Tulio FA de Lima e Moura, MedeirosACD, GomesAPB, AragaoCFS. Journal of Thermal Analysis and Calorimetry2014,115; 2311-2318.
2. Totonchy MB, ChiuMW, Dermatologic Clinics, **Error! Hyperlink reference not valid.**2014,32; 399–413.
3. Huijuan MA, Qiang MA, Wentao LI, Xianshuang MENG, Jingrui LI, Hua BAI, YangJIAO, Xiaoli ZHANG.J Chinese Chromatogr, 2013,31(5); 416-422.
4. HannuselaM ,Karvonen J. British journal of Dermatology 1978,99; 703.
5. FiitfiinenV, Taskinen J, Arch Dermatol Res 1981,270; 157-158.
6. Orion Corporation, Research Laboratories, P.O Box 19, SF-00101 Helsinki 10, Finland.
7. Frisch M.J, TrucksGW,Schlegel HB, Scuseria GE et al, Gaussian 03W,Revision A 02, Inc., Wallingford, CT, 2004.
8. Becke AD, J. Chem. Phys. 1992,97; 9173–9177.
9. Becke AD, J. Chem. Phys. 1993,98; 5648–5652.
10. Jamroz MH, Vibrational Energy Distribution Analysis, VEDA 4, Warsaw, 2004.
11. Varsanyi G, Assignments for Vibrational Spectra of Seven Hundred Benzene.
12. Keresztury G, Holly S, Varga J, Besenyei G, Wang AY, DurigJR, Spectrochim.Acta A 1993,49; 2007–2026.
13. Fast PL, Corchado J, Sanches ML, Truhlar DG, J. Phys. Chem. A 1999,103; 3139–3143.
14. Frisch A, Dennington RD, Keith TD, et al., Gauss View version 4.1 User Manual, Gaussian, Wallingford, Conn, USA, 2007.
15. Peesole RL, Shield LD, Mcwillam IC, Modern Methods of Chemical Analysis, Wiley, New York, 1976.
16. Subashchandrabose S, Krishnan AR, Saleem H, Parameswari R, Sundaraganesan N, Thanikachalam V, Manikandan G, Spectrochim. ActaA,2010,77; 877–884.
17. James C, Amal Raj A, Reghunathan R, Hubert Joe I, Jayakumar VS, J. Raman Spectrosc. 2006,37; 1381–1392.
18. Fukui K, Yonezawa T, Shingu H, J. Chem. Phys.1952,20; 722–725.
19. Padmaja,L, Ravi Kumar C, Sajjan D, Hubert Joe I, Jayakumar VS, Pettit GR, J. Raman Spectrosc. 2009,40; 419–428.
20. Sagdinc S, Pir H, Spectrochim. Acta2009,73A; 181–187.

\*\*\*\*\*